Tuijin Jishu/Journal of Propulsion Technology
ISSN: 1001-4055
Vol. 45 No. 3 (2024)

Experimental Study of a Cross-Flow Indirect Evaporative Cooling System

Abdalazeem Adam [1*], Weifeng He [2], Dong Han [3], Omer Musa [4]
[1] *College of Energy and Power Engineering, Nanjing University of Aeronautics and Astronautics, Nanjing, Jiangsu, China*

Abstract:- In this paper, an experiment was conducted to study the effectiveness of a cross-flow indirect evaporative cooler (IEC). The experiment aimed to investigate the influence of intake air velocity, inlet temperature, and secondary air humidity on the performance of the IEC. The key findings revealed that higher inlet temperatures led to a significant decrease in air temperature in both channels, with a notable temperature reduction from 40.6 °C to 29.21 °C and 26.42 °C for the secondary air. Conversely, at an inlet temperature of 27.5 °C, the temperature difference was only 3.58 °C. Lower inlet temperatures showed less pronounced temperature differences. Furthermore, increasing the secondary air velocity positively impacted the system's performance, resulting in lower outlet temperatures at a velocity of 2 m/s. Conversely, an increase in primary air velocity was found to have a detrimental effect on the system's performance.

Keywords*:* Wettability factor, Indirect evaporative cooling system, Cross-flow configuration, heat and mass exchanger.

1. Introduction

Indirect evaporative cooling (IEC) systems have gained significant attention in the field of thermal comfort and energy efficiency in buildings. These systems utilize the principle of evaporative cooling to provide cooling without adding moisture to the indoor air, making them suitable for hot and dry climates [1]. This innovative technology offers flexibility and can be effectively employed across various HVAC applications, including data centers, sports complexes, and commercial buildings [2]. The IEC system can be implemented in several configurations: conventional IEC devices, typical IEC units within a dry drive system, renewable IEC systems in a wet configuration, and energy-efficient units integrated with traditional cooling systems [3], [4]. Various IEC units, such as flat plate, irregular plate, and tube types, are available, each designed to meet specific cooling requirements [5]. Flat plate IEC units, for example, can be categorized into single, dual, or multistage designs [6]. Depending on the system's needs and design, these units can also be arranged in different flow configurations, including crossflow, parallel flow, or counterflow [7]. The adoption of IEC systems is driven by their ability to efficiently address building cooling demands, reduce chlorofluorocarbon (CFC) emissions, and lessen reliance on conventional air conditioning methods [8]. As a result, IEC technology represents a promising alternative for improving indoor climate control while contributing to environmental sustainability.

Researchers have been focusing on experimental and numerical investigations to optimize the performance of IEC systems, considering factors such as heat transfer efficiency, modeling, optimization, and sustainability. Various flow characteristics and operational parameters influence the effectiveness of a cross-flow IEC system. Researchers have extensively studied the impact of different flow parameters and operating conditions on the performance of IEC systems [9]. The performance of IEC systems is typically defined in terms of parameters such as cooling capacity and coefficient of performance [10]. Numerical modeling has been used to analyze the heat and mass transfer characteristics within plate-type cross-flow indirect cooling systems, highlighting the importance of these factors on system performance [11]. Additionally, studies have been conducted on optimizing combined thermoelectric systems and regenerative cross-flow systems under various operating conditions, emphasizing the significance of cross-flow heat exchangers in IEC [12]. Experimental and analytical studies have also been conducted to investigate the sensitivity of key design and operational parameters on the cooling performance of IEC systems [13]. The geometry of heat exchanger plates has been shown to impact IEC systems' performance [14] significantly. Furthermore, performance prediction and optimization of cross-flow indirect evaporative coolers have been a focus of recent research, highlighting the environmentally friendly nature of these systems [15]. The wettability characteristic of wet channels has been identified as a crucial factor in the cooling performance of indirect evaporative coolers, emphasizing the importance of flow characteristics in system design [16]. A detailed experimental investigation of system performance under various outdoor air temperatures and airflow rates has provided valuable insights into the energy-efficient design of IEC systems [17].

In addition, the research on cross-flow IEC systems has seen significant advancements in recent years. Adam et al. [11] focused on the numerical modeling of heat and mass transfer characteristics within a plate-type cross-flow indirect cooling system, considering the impact of the surface wettability factor. Guo et al. [18] developed a mathematical model based on the condensation area ratio to analyze the heat transfer capacity of IEC systems. Liu et al. [19] introduced an enthalpy efficiency index to evaluate an indirect evaporative cooler's total heat transfer efficiency. Katramiz et al. [20] investigated the performance of a hybrid passive cooling system combining diurnal radiative cooling and an IEC system in a hot climate. Ren et al. [21] developed a mathematical model for cross-flow energy-recovered IEC system-assisted liquid desiccant dehumidifiers, focusing on the wetness coefficient's effect on heat exchanger effectiveness and dehumidification efficiency. Harrouz et al. [22] proposed a passive ventilation and air conditioning system integrating a cross-flow dew point indirect evaporative cooler for office space in a hot climate. Yang et al. [23] and Sajjad et al. [24] have reviewed the research progress in IEC technology, highlighting this cooling approach's energy-efficient and eco-friendly nature. Additionally, Lee et al. [25] conducted a performance analysis of a solid desiccant cooling system for residential air conditioning, showcasing the diverse range of cooling technologies available in the literature. Overall, the literature on cross-flow IEC systems demonstrates a growing interest in improving heat and mass transfer efficiency, evaluating system performance, and exploring hybrid cooling solutions for different climate conditions [26]. Also, the literature suggests that the effectiveness of cross-flow IEC systems is influenced by a combination of flow characteristics and operational parameters, highlighting the importance of optimizing these factors for enhanced system performance. These studies contribute to the development of more sustainable and effective cooling technologies. The performance of the IEC system is crucial in determining the overall system efficiency, scale, and cost. As a result, extensive research has been conducted to investigate how different flow parameters, flow patterns, and exchanger dimensions affect the performance of the IEC system through simulations and experiments. However, experimental studies remain needed to explore the impact of flow parameters on IEC performance.

This study built and tested a cross-flow IEC unit to assess its efficiency and address existing research gaps. The IEC system includes a flat plate serving as a heat and mass exchanger, a water tank, water spray nozzles positioned in the upper portion of the plate, and a circulating pump. The system has undergone multiple testing procedures. The effects of intake air velocity, intake temperature, and secondary air humidity on performance were examined. The findings of this research provide practical insights into the ideal operating parameters for achieving high operational efficiency and the perfect cooler design specifications, which can be directly applied in the field of refrigeration technology, HVAC applications, and energy-efficient cooling systems.

2. Experimental Setup

The fabricated cross-flow indirect evaporative cooler system setup laboratory was meticulously designed and constructed. The IEC system comprises flat plates that act as heat and mass exchangers, a water tank, water spray nozzles located at the upper part of the plate, and a pump that circulates water. The schematic of the IEC module was stacked together utilizing two air passes, including dry and wet channels. A thin stainless-steel flat plate divided the dry and wet channels. Both channels were supported by plastic corrugated sheets that served as primary and secondary air guiders, as seen graphically in Fig. 1.

Figure 1 Photographic view of the experimental unit.

The geometric characteristics of dry channels, wet channels, and the plate are presented in Table I. As shown in Fig. 1, the air intake module consists of a long extension duct with an attached fan, air heater, and humidifier. The air heater and humidifier control the temperature and humidity of the secondary air entering the IEC. The fan was controlled by a variable speed controller, which varied the input airflow rate into the IEC module. Similarly, the primary air duct includes a fan with a variable speed controller positioned in a long extension duct to adjust the intake air. A circulating water system was built to produce uniform wetting conditions for the IEC's wet channels. The system includes a lower tank, a water distributor, a circulating water pipe, and a water pump with a controller. The spray pipe was placed above the top of HMX. Water sprayed equally along the horizontal direction of the wet channel surface as it flowed down to the connecting water sink. Table II lists the equipment for measuring temperature, relative humidity, and velocity.

The IEC system's performance was tested under different operating conditions through experiments. An air heating device and humidifier were used to vary the air temperature and humidity, simulating outside conditions. The system involves two air streams: primary and secondary air. A water film forms over the plate surface from water entering the heat exchanger's wet channel or internal spraying. The water removes latent heat and transfers it to the airstream as the secondary air passes over the water film layer. The cooled water layer absorbs heat from the next plate. When the primary air temperature exceeds the plate's temperature, heat is transferred from the air in the duct to the plate and then to the secondary air and water film as sensible heat. The dynamic parameters are detailed in Table I.

Table I Geometric characteristics of the test unit and ranges of dynamic parameters.

Parameter	Range	Units	Geometry	Value	Units
Units Primary air inlet temperature	27.5 - 41	°C	Primary air gap	10	mm
Secondary air inlet temperature	25.6 - 30	°C	Secondary air gap	10	mm
Secondary air inlet velocity	1 - 2	m/s	Plate length	600	mm
Primary air inlet velocity	1 - 2	m/s	Plate width	600	mm
Inlet air relative humidity	33 - 60	%	Plate thickness	0.4	mm
Water inlet temperature	23 - 27	°C	Channel pairs	2	-

Table II Experimental instrumentations applied in measuring parameters.

Measured parameters	Apparatus	Measurement range	Accuracy
Air temperature	Temperature sensor Model: TMC6-HD HOBO	0 − 100 °C	±0.15 ˚C
Relative Humidity	RH and temperature sensor: RH-USB OMEGA	RH 2 − 98%	Relative Humidity ±3%
Water temperature	Temperature sensor Model: TMC6-HD HOBO	0 − 100	±0.15˚C
Air velocity	Hotwire anemometer Model: Testo-425	0 − 20 m/s	±0.03 m/s

3. Performance Indicator of IEC System

The efficiency of the primary air stream in a non-condensing state was computed based on the collected temperature data. Equation 1 outlines the wet-bulb efficiency [18].

$$\varepsilon_{wb} = \frac{t_{p,i} - t_{p,o}}{t_{p,i} - t_{wb}} \tag{1}$$

The performance of an IEC system depends significantly on its cooling capacity, which is primarily determined by the sensible heat transferred from the primary to the secondary airflow (as mentioned in reference [19]). Equation 2 defines the sensible cooling capacity of the IEC system:

$$Q_c = \dot{m}_p \cdot c_{p,a}(t_{p,i} - t_{p,o}) \tag{2}$$

The coefficient of performance (COP) indicates the ratio of cooling or heating output to the power input, which can be expressed as:

$$COP = \frac{Q_c}{P} \tag{3}$$

Where $P = P_{pump} + P_{instruments} + P_{fan}$ is the power input of the system.

4. Experiment Results and Discussion

In this section, the experimental results of the test unit are presented and discussed in detail. As mentioned in the previous section, the wettability factor is about 0.6, and the other inlet and operating conditions are summarized in Table I.

A. Effect of supply air velocity

In Fig. 2, the effect of the secondary air velocity is evaluated; all tests are performed at the velocity range (1-2) m/s, and the other operating conditions remain constant. The inlet temperature of the secondary air is 26 and

27.86°C for primary air, the humidity is 34%, and the primary air velocity is 1 m/s. Fig. 2(a) shows the outlet temperature of the two channels versus different intake velocities. It can be seen that the temperature decreases when the velocity rises. The minimum value for the temperature at the exit is obtained when the velocity is 2 m/s. Because of the increase in air velocity, the wet channel will enhance the evaporation process, resulting in more cooling. Also, the efficiency has been evaluated, as illustrated in Fig. 2(b). Notably, the efficiency increased when the velocity rose. In contrast, COP decreases by raising the velocity because system losses such as pressure drop, friction, and fan power increase. Finally, it is possible to state that the unit outlet temperature mainly depends on the secondary air inlet velocity.

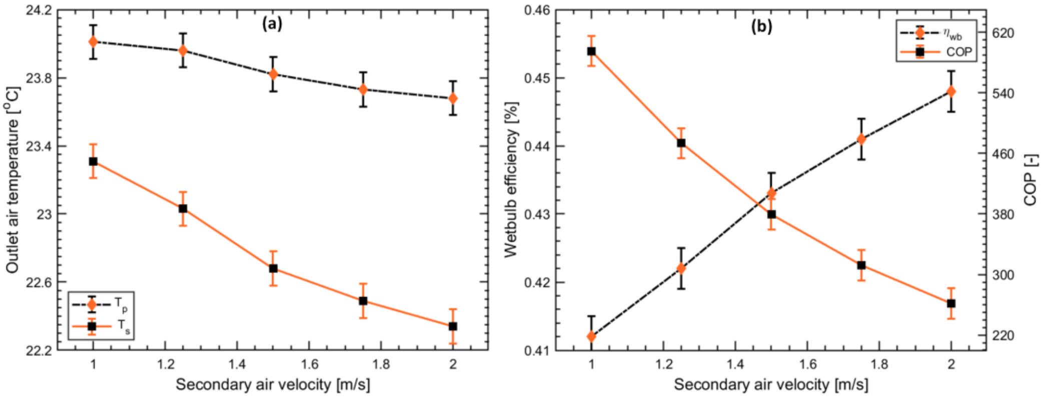

Figure 2 shows the effect of secondary air velocity: (a) Average outlet temperature, (b) wet-bulb efficiency, and COP.

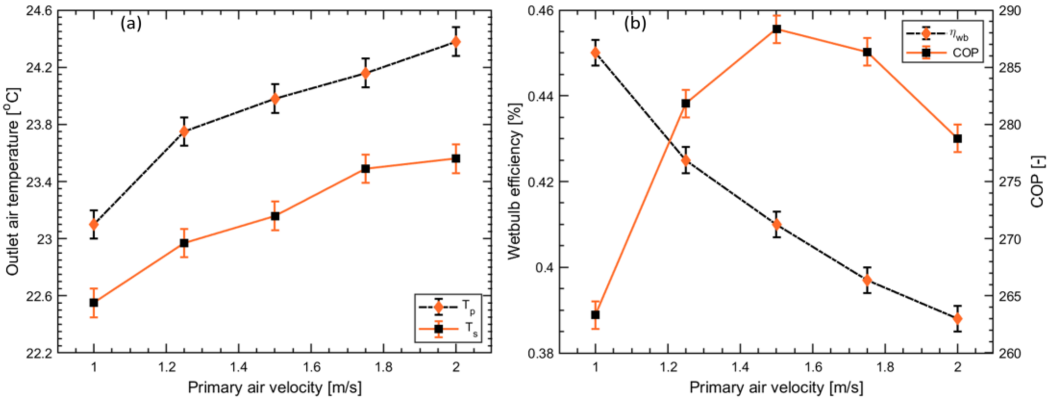

Figure 3 shows the effect of primary air velocity: (a) Average outlet temperature, (b) wet-bulb efficiency, and COP.

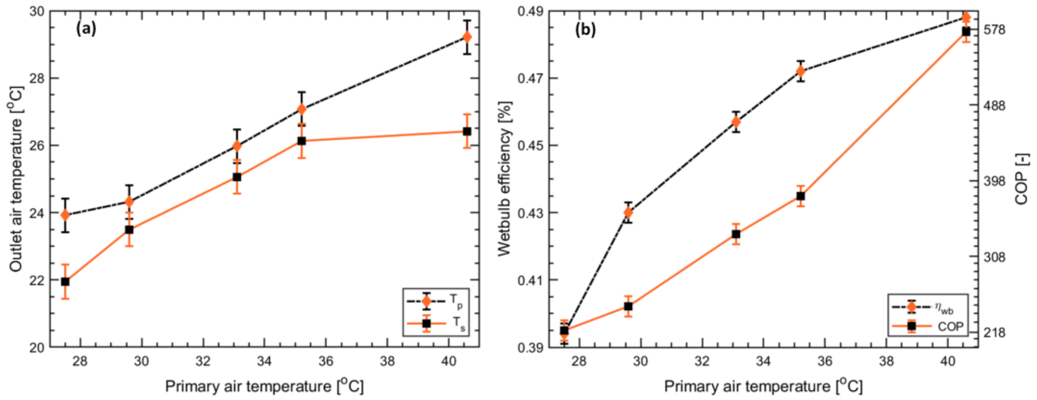

Figure 4 shows the effect of primary air temperature: (a) Average outlet temperature, (b) wet-bulb efficiency, and COP.

Increasing the secondary air velocity improves the system's performance, whereas a higher primary air velocity has a detrimental effect. In our experiments, we varied the air velocity between 1 m/s and 2 m/s in steps of 0.25 m/s, while keeping other conditions constant.

Figure 3(a) shows the average temperatures of both primary and secondary air as a function of the input air velocity. As the primary air velocity was increased from 1 m/s to 2 m/s, the temperature rose from 23.1°C to 24.38°C. This temperature increase is due to the higher mass flow rate of primary air, which shortens the time available for heat exchange with the wet channel. The secondary air exhibited a similar pattern.

The decline in wet-bulb efficiency was linked to the higher primary air mass flow rate, which resulted in a higher outlet air temperature. Figure 3(b) highlights that both wet-bulb efficiency and the coefficient of performance (COP) decrease as the primary air velocity increases. Therefore, optimizing the inlet air velocity is essential for maximizing system efficiency.

Effect of primary air temperature

In this experiment, the primary air inlet temperature was increased using an air heater, and five different test points were obtained. Fig. 4(a) depicts the outlet's primary and secondary air temperature change for various intake air temperatures. The air temperature drops significantly in two channels when the intake temperature is high. When the intake air temperature is low, it can be seen to decline lower than when the inlet air temperature is high. For example, at intake air temperature was 40.6 °C, the temperature dropped quickly to 29.21 °C and 26.42 °C for secondary air, but when the entry temperature was 27.5 °C, the temperature was different by just about 3.58 °C. On the other hand, the temperature at the outflow did not alter significantly.

In the graph labeled Fig. 4(b), the wet-bulb efficiency and coefficient of performance (COP) were analyzed at different primary air inlet temperatures. The results showed that both the efficiency and COP increased as the air inlet temperature rose. Specifically, when the temperature reached 40.6 °C, the wet-bulb efficiency reached 48.8%, and the COP increased to 574.62. This improvement in cooling performance can be attributed to the enhanced heat transfer between the two channels due to the higher input temperature.

Effect of secondary air humidity

During the experiments to study the effects of working air humidity using an adiabatic humidifier, the relative humidity varied between 34% and 60%. All other flow factors, such as air velocity and intake temperatures, remained consistent for both airstreams throughout the tests.

The average temperature at the exit of the primary and the secondary is shown in Fig. 5(a). The highest values for the outlet air temperature were 25.94 °C and 25.02 °C, achieved when the relative humidity was 60%. As observed, raising the working air humidity has a detrimental impact on the system’s cooling performance. This phenomenon occurs because when humid air enters the wet duct, it cannot carry additional water vapor. This limitation impacts the evaporative cooling process and the heat exchange between the two channels. Figure 5(b) illustrates this effect by comparing wet-bulb efficiency and the coefficient of performance (COP) at various relative humidity levels. As relative humidity increased from 34% to 60%, the COP decreased from 205.5 to 134.1. This reduction in COP is due to the higher wet-bulb temperature at the inlet, which indicates that wet-bulb efficiency improves with increasing humidity.

The impact of the secondary air humidity in the contour in Fig. 6 shows another experiment’s results on a hot and humid day. The temperature was 28.5 °C for both channels, while the velocity was 2m/s in the wet duct and 1m/s for the dry one and the water at room temperature. A temperature decrease in the flow direction and the wetting effect can be seen on the plate surface. In some places, there is no water; therefore, the heat is transferred between the two air streams, resulting in even temperature distribution in the same line in the flow direction. Also, it can be seen that the decrease is minimal, which is 3 °C for the dry channel and 4 °C for the wet channel.

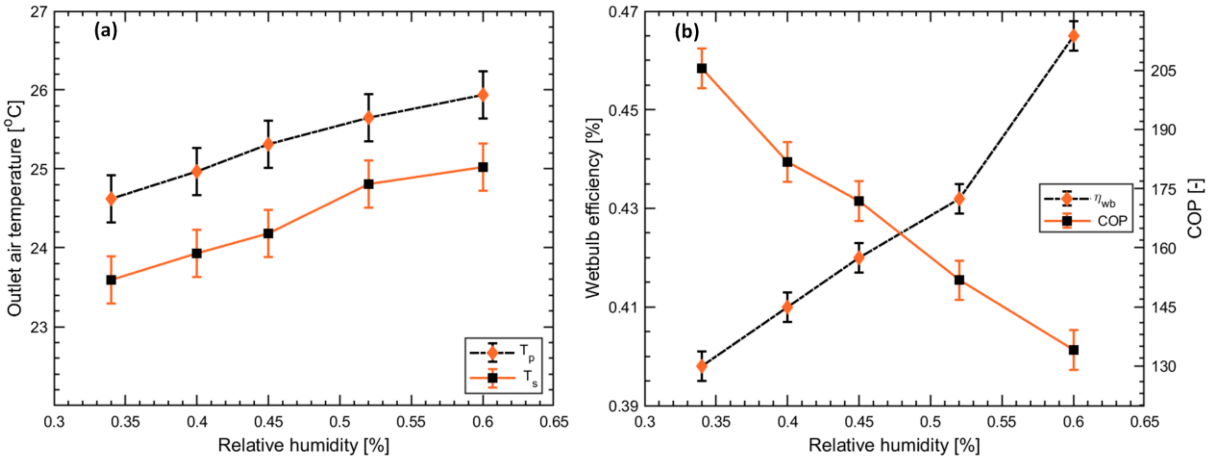

Figure 5 shows the effect of secondary air humidity: (a) Average outlet temperature, (b) wet-bulb efficiency, and COP.

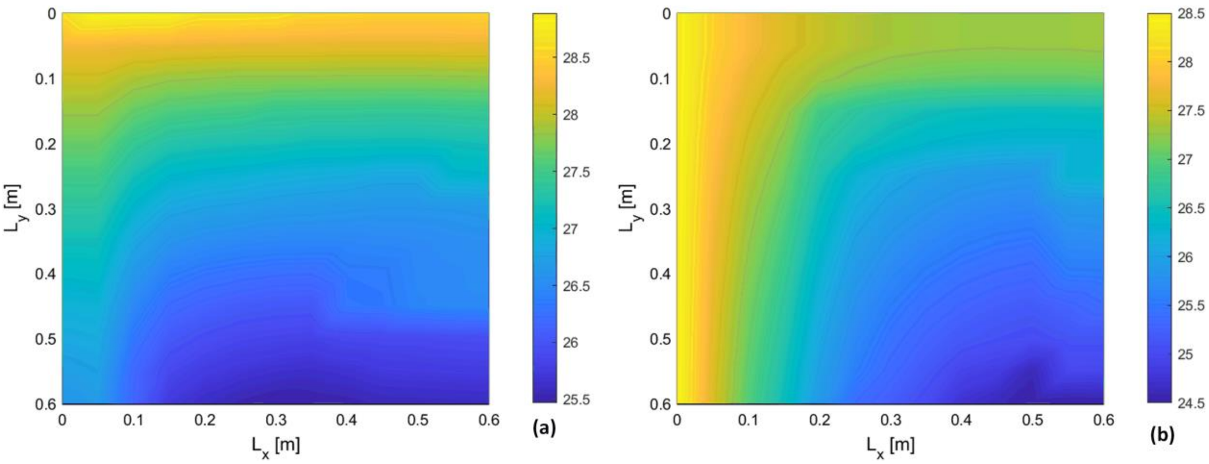

Figure 6 contour of the temperature at high inlet humidity.

5. Conclusions

In this study, we developed a cross-flow indirect evaporative cooler (IEC) to investigate how various flow parameters affect its performance, focusing on outlet temperature, wet-bulb efficiency, and coefficient of performance. Through a series of experiments conducted under different flow conditions, we analyzed the impacts of factors such as air velocity, intake temperature, and secondary air humidity. These experimental results were then used to validate an existing numerical model. The key findings are summarized as follows:

- Secondary Air Velocity: An increase in secondary air velocity results in a lower exit temperature, with the lowest temperature achieved at a velocity of 2 m/s. Higher secondary air velocity improves the evaporation rate in the wet channel, thereby enhancing cooling efficiency. However, higher primary air velocity tends to degrade system performance.
- Intake Temperature: At elevated intake temperatures, a substantial reduction in air temperature is observed in both channels. For example, when the intake temperature was 40.6°C, the secondary air temperature fell to 29.21°C, and the primary air temperature dropped to 26.42°C. In comparison, with an intake temperature of 27.5°C, the temperature difference was only 3.58°C. Higher intake temperatures facilitate better heat transfer between channels, improving cooling.
- Inlet Relative Humidity: Reducing the relative humidity of the inlet air results in better cooling performance across all evaluated metrics—outlet temperature, wet-bulb efficiency, and coefficient of performance.

References

[1] X. Zhao, J. Li, S. Riffat, Numerical study of a novel counter-flow heat and mass exchanger for dew point evaporative cooling, Applied Thermal Engineering 28 (14-15) (2008) 1942–1951.

[2] M. H. Mahmood, M. Sultan, T. Miyazaki, S. Koyama, V. S. Maisotsenko, Overview of the maisotsenko cycle–a way towards dew point evaporative cooling, Renewable and sustainable energy reviews 66 (2016) 537–555.

[3] B. Porumb, P. Ungures¸an, L. F. Tutunaru, A. S¸ erban, M. Baˇlan, A review of indirect evaporative cooling operating conditions and performances, Energy Procedia 85 (2016) 452–460.

[4] P. Xu, X. Ma, T. M. Diallo, X. Zhao, K. Fancey, D. Li, H. Chen, Numerical investigation of the energy performance of a guideless irregular heat and mass exchanger with corrugated heat transfer surface for dew point cooling, Energy 109 (2016) 803 – 817.

[5] X. Cui, X. Yang, Q. Kong, X. Meng, L. Jin, Performance evaluation and comparison of multistage indirect evaporative cooling systems in two operation modes, International Journal of Energy Research 44 (12) (2020) 9298–9308.

[6] D. Pandelidis, A. Cichon´, A. Pacak, S. Anisimov, P. Dra¸g, Counter-flow indirect evaporative cooler for heat recovery in the temperate climate, Energy 165 (2018) 877–894.

[7] D. Pandelidis, A. Cichon´, A. Pacak, S. Anisimov, P. Dra¸g, Performance comparison between counter- and cross-flow indirect evaporative coolers for heat recovery in air conditioning systems in the presence of condensation in the product air channels, International Journal of Heat and Mass Transfer 130 (2019) 757–777.

[8] Pacak, A., & Worek, W. (2021). Review of dew point evaporative cooling technology for air conditioning applications. Applied Sciences, 11(3), 934.

[9] Adam, A., Han, D., He, W., & Amidpour, M. (2021). Analysis of indirect evaporative cooler performance under various heat and mass exchanger dimensions and flow parameters. International Journal of Heat and Mass Transfer, 176, 121299.

[10] Jamil, M. A., Xu, B. B., Dala, L., Sultan, M., Jie, L., & Shahzad, M. W. (2021). Experimental and normalized sensitivity based numerical analyses of a novel humidifier-assisted highly efficient indirect evaporative cooler. International Communications in Heat and Mass Transfer, 125, 105327.

[11] Adam, A., Han, D., He, W., & Chen, J. (2021). Numerical analysis of cross-flow plate type indirect evaporative cooler: Modeling and parametric analysis. Applied Thermal Engineering, 185, 116379.

[12] Zhou, Y., Zhang, T., Wang, F., & Yu, Y. (2020). Numerical study and optimization of a combined thermoelectric assisted indirect evaporative cooling system. Journal of Thermal science, 29, 1345-1354.

[13] Dizaji, H. S., Hu, E. J., Chen, L., & Pourhedayat, S. (2020). Analytical/experimental sensitivity study of key design and operational parameters of perforated Maisotsenko cooler based on novel wet-surface theory. Applied Energy, 262, 114557.

[14] Jamil, M. A., Imtiaz, N., Ng, K. C., Xu, B. B., Yaqoob, H., Sultan, M., & Shahzad, M. W. (2023). Experimental and parametric sensitivity analysis of a novel indirect evaporative cooler for greener cooling. Thermal Science and Engineering Progress, 42, 101887.

[15] Shi, W., Yang, H., Ma, X., & Liu, X. (2023). Performance prediction and optimization of cross-flow indirect evaporative cooler by regression model based on response surface methodology. Energy, 283, 128636.

[16] Sun, T., Huang, X., Qu, Y., Wang, F., & Chen, Y. (2020). Theoretical and experimental study on heat and mass transfer of a porous ceramic tube type indirect evaporative cooler. Applied Thermal Engineering, 173, 115211.

[17] Jamil, M. A., Shahzad, M. W., Xu, B. B., Imran, M., Ng, K. C., Zubair, S. M., ... & Worek, W. M. (2023). Energy-efficient indirect evaporative cooler design framework: An experimental and numerical study. Energy Conversion and Management, 292, 117377.

[18] Guo, C., Liu, Q., Zheng, B., You, Y., & Li, Y. (2020). Development of model based on condensation area ratio and effect on heat transfer capacity of indirect evaporative cooling. Applied Thermal Engineering, 164, 114557.

[19] Liu, Q., Guo, C., Ma, X., You, Y., & Li, Y. (2020). Experimental study on total heat transfer efficiency evaluation of an indirect evaporative cooler. Applied Thermal Engineering, 174, 115287.
[20] Katramiz, E., Al Jebaei, H., Alotaibi, S., Chakroun, W., Ghaddar, N., & Ghali, K. (2020). Sustainable cooling system for Kuwait hot climate combining diurnal radiative cooling and indirect evaporative cooling system. Energy, 213, 119045.
[21] Ren, Y., Guo, C., Lv, J., Xu, J., Dong, S., Meng, D., ... & Guo, S. (2021). Experimental study on a cross-flow energy recovered indirect evaporative cooling (ERIEC)-assisted liquid desiccant dehumidifier (LDD) with improved spraying nozzle and surface wetness. Science and Technology for the Built Environment, 27(7), 903-916.
[22] Harrouz, J. P., Ghali, K., & Ghaddar, N. (2021, June). A Passive Ventilation and Air Conditioning System for an Office Space In Hot Climate. In Heat Transfer Summer Conference (Vol. 84874, p. V001T01A005). American Society of Mechanical Engineers.
[23] Yang, H., Shi, W., Chen, Y., & Min, Y. (2021). Research development of indirect evaporative cooling technology: An updated review. Renewable and Sustainable Energy Reviews, 145, 111082.
[24] Sajjad, U., Abbas, N., Hamid, K., Abbas, S., Hussain, I., Ammar, S. M., ... & Wang, C. C. (2021). A review of recent advances in indirect evaporative cooling technology. International Communications in Heat and Mass Transfer, 122, 105140.
[25] Lee, Y., Park, S., & Kang, S. (2021). Performance analysis of a solid desiccant cooling system for a residential air conditioning system. Applied Thermal Engineering, 182, 116091.
[26] Zhou, Y., Yan, Z., Dai, Q., & Yu, Y. (2021). Experimental and numerical evaluation of a two-stage indirect/thermoelectric assisted direct evaporative cooling system. Energy Conversion and Management, 248, 114780.